Composites: Part B xxx (2012) xxx–xxx

Contents lists available at SciVerse ScienceDirect

Composites: Part B

journal homepage: www.elsevier.com/locate/compositesb

# Preparation, characterization and thermoelectricity of ATT/$TiO_2$/PANI nano-composites doped with different acids

Lulu Chen [a,1], Yun Zhai [b,1], Hongyan Ding [a,b,*], Guanghong Zhou [a], Yufu Zhu [a], David Hui [b]

[a] Jiangsu Provincial Key Lab for Interventional Medical Devices, Huaiyin Institute of Technology, Huaian 223003, China
[b] Department of Mechanical Engineering, University of New Orleans, LA 71048, USA

ARTICLE INFO

*Article history:*
Received 15 December 2011
Accepted 10 February 2012
Available online xxxx

*Keywords:*
A. Polymer-matrix composites (PMCs)
A. Nano-structures
B. Thermal properties
Doping-acid

ABSTRACT

ATT/$TiO_2$/PANI (ATOP) nano-composites were synthesized by *in situ* polymerization under different doping-acids (HCl, sulfosalicylic acid (SSA), HCl + SSA dual acids, $HClO_4$) in the presence of ATT/$TiO_2$ nano-particles. The effects of various doping-acids on the microstructure, morphology, thermal stability and thermoelectric properties were also discussed. The results show that the ATOP nano-composites doped with HCl + SSA dual acids present a better thermoelectric properties, combined with high electrical conductivity, Seebeck coefficient, and low thermal conductivity. A higher value of ZT is kept in the range of 323–373 K for the HCl + SSA dual acids doped ATOP nano-composites. The results indicate that the HCl + SSA dual acids doped ATOP nano-composites can be available for power generation with low temperature heat, e.g. exhaust gas, terrestrial heat, solar energy, etc.



## 1. Introduction

The thermoelectric effect refers to phenomena in which a temperature gradient creates an electric potential and vice versa, using the electrical carriers, electrons and holes, in the solid state devices as the working fluids with no moving parts [1,2]. This offers many distinguished characteristics such as that they are environmentally friendly, quiet, compact, light and scalable [3–5]. Though all materials have a nonzero thermoelectric effect, in most materials it is too small to be useful. A good thermoelectric material is the one with a high Seebeck coefficient, a high electrical conductivity, and a low thermal conductivity [6]. As all the three properties are interconnected, it has proved impossible to raise the value of the figure-of-merit (*ZT*) to a higher level till recently [7]. Thus far, the best thermoelectric materials are found in heavily doped semiconductors due to the fact that insulators have poor electrical conductivity and metals have low Seebeck coefficient. While among the most promising transition semiconductors, titanium dioxide ($TiO_2$) stands out because of its special chemical and physical properties as a thermoelectric material [8]. However, low value of *ZT* and other unmatched mechanical properties limit its application.

Polyaniline (PANI) is one of the most important conducting polymers because of its high environmental stability, low cost and reversible control of its conductivity [9]. Recently, polymer/inorganic composites have received much attention due to their independent electrical, optical, and mechanical properties [10–12]. The combination of conducting polymers and semiconducting inorganic materials with the properties of semiconducting inorganic particles has brought new prospects for applications [13]. Usually, the strong interaction between eigenstate PANI rigid chains leads to low conductivity. However, $H^+$ can be easily poured into the PANI molecular chains, and thus increases the level of charge delocalization and improves the conductivity. Up to now, various protonic acids have been used as dopants during the process of synthesis. Commonly, these protonic acids were inorganic acids (e.g. HCl, $H_2SO_4$, $H_3PO_4$, and $HClO_4$) [14–16]. Recently, it has been reported that PANI doped with organic acids, such as benzenesulfonic acid (BSA) [17], sulfosalicylic acid (SSA) [18], camphorsulfonic acid (CSA) [19] and p-styrenesulfonic acid (PSSA) [20], are prone to improve their thermal stability.

In our previous work, $TiO_2$ nano-particles have been encapsulated into shell of conducting PANI giving rise to a host of nano-composites [21]. The problem encountered is aggregation of nano-particles because of its higher surface energy [22]. Attapulgite (hereinafter referred to as ATT), a species of hydrated manesium aluminum silicate non-metallic mineral [$(H_2O)_4(Mg,Al,Fe)_5(OH)_2Si_8O_{20}{\cdot}4H_2O$] with commonly a fibrous morphology, is characterized by a porous crystalline structure containing tetrahedral layers alloyed together along longitudinal sideline chains [23]. Presently ATT has been widely used as adsorbents, adhesives, and catalyst supports, owing to its unique structure and considerable textual properties [24,25].

* Corresponding author at: Jiangsu Provincial Key Lab for Interventional Medical Devices, Huaiyin Institute of Technology, Huaian 223003, China. Tel.: +86 517 83559130; fax: +86 517 83559150.
*E-mail address:* nanhang1227@gmail.com (H. Ding).
[1] Authors contributed equally.

1359-8368/$ - see front matter © 2012 Elsevier Ltd. All rights reserved.
doi:10.1016/j.compositesb.2012.02.028

In this work, ATT/$TiO_2$ (ATO) nano-particles were first prepared by heterogeneous nucleation method; then, ATT/$TiO_2$/PANI (ATOP) was synthesized by *in situ* polymerization in the presence of ATO nano-particles under various acids (HCl, SSA, HCl + SSA dual acid, $HClO_4$). The ATT was used as support to reduce the aggregation and improve the dispersibility of nano-particles, and reduce the thermal conductivity simultaneously. We systematically investigated the effects of various acid-doping on the morphology, crystallographic, thermal stability and thermoelectric properties of ATOP nano-composites.

## 2. Experimental

### 2.1. Synthesis of ATT/$TiO_2$/PANI nano-composites

Fig. 1 shows the flow chart of preparation on the ATOP nano-composites. The ATT/$TiO_2$ (ATO) nano-particles were synthesized firstly. 10 ml Tetrabutyl titanate ($Ti(OBu)_4$) was dissolved into 100 ml absolute alcohol ($C_2H_5OH$) solution with a smidgeon of triethanolamine (about 0.2 ml) by vigorous mechanical stirring (namely solution A). 1.3 ml $HNO_3$ in 2 ml distilled water was added to 10 ml absolute alcohol (namely solution B). Then solution B was added dropwise to solution A with vigorous stirring for 1 h at room temperature. After mixing uniformly, transparent, stable and flaxen $TiO_2$ sol was added dropwise to the pure ATT suspension with sonic stirring for 1 h. After aging for 4 h in the air, the mixture was washed with distilled water. The resulting solid was dried at 353 K for 24 h and subsequently calcined at 723 K for 3 h; then the solid was ground into ATO nano-particles. The second step was to fabricate ATT/$TiO_2$/PANI (ATOP) nano-composites, which were synthesized by the oxidation of precursor with ammonium peroxydi-sulfate (APS) as oxidant. ATO (0.64 g) was dispersed into 40 ml 1.0 M acid solution (HCl, SSA, HCl + SSA dual acid, $HClO_4$) by sonication respectively. Then 1.86 g aniline and little surfactant hexadecyl trimethyl ammonium bromide (CTAB) were added into ATO acid solution under protection of nitrogen atmosphere. The molar ration of aniline/surfactant was taken as 10. After 30 min, APS (3.65 g) in 20 ml 1.0 M acid solution was added dropwise to this mixture. Polymerization was carried out at 273 K under nitrogen atmosphere with controlled stirring for 5 h. Dark green ATOP nano-composites was filtered and washed with distilled water before it is dried at 353 K under vacuum for 24 h.

### 2.2. Characterization

The surface morphology of the ATOP nano-composites was examined by a Hitachi S-3000 N scanning electron microscope (SEM). X-ray powder diffraction were performed on a D8 Advance diffractometer (XRD) using Cu–$K_\alpha$ radiation ($\lambda$ = 0.15405 nm). FTIR spectra were recorded using a Nicolet 5700 Fourier Transform Infrared Spectrometer in a dry-nitrogen atmosphere. Thermogravimetric analysis was performed with NETZSCH STA409PC thermal analyzer at a heating rate of 15 K/min from 298 K to 473 K under a nitrogen atmosphere. The thermal conductivity of the composites was measured using EKO HC-110 thermal conductivity test meter, which is based on a steady-state heat flux technique. The powder samples were in the form of compressed pellet ($\Phi$22 mm × 2 mm) for the thermoelectric related measurements. Electrical conductivity was measured by ST2253 four-probe tester. The Seebeck coefficient was tested on BHTE-08 Seebeck Measurement System.

## 3. Results and discussions

Fig. 2a–d shows the SEM micrographs of HCl, SSA, HCl + SSA and $HClO_4$ doped ATOP nano-composites, respectively. Hereinafter these samples were denoted as ATOP-1, ATOP-2, ATOP-3, and ATOP-4. One can see that all the samples are of rod-like structure

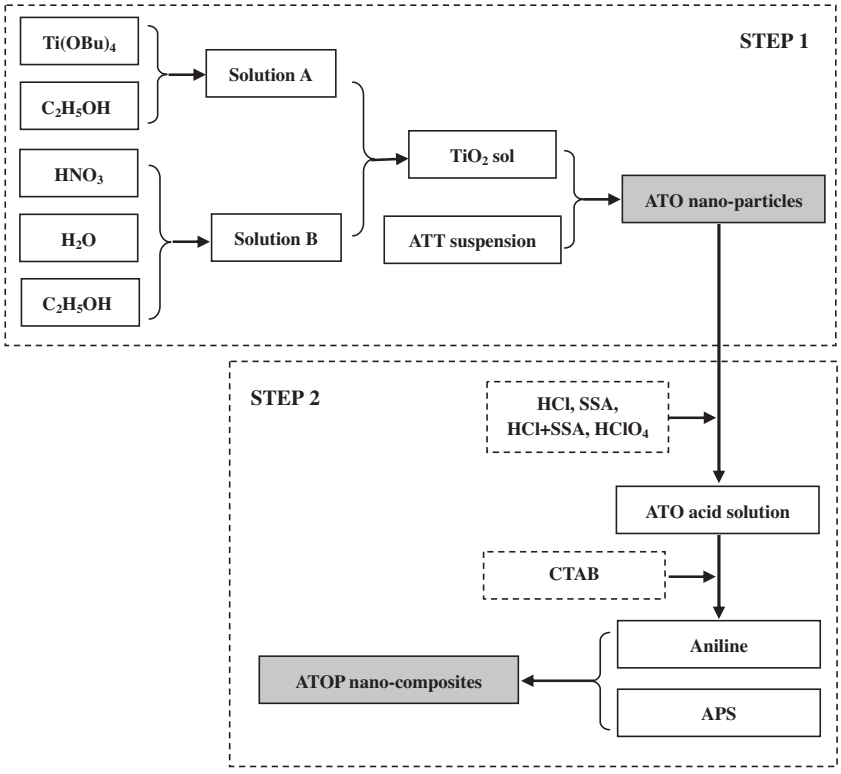


**Fig. 1.** Flow chart of preparation on the ATOP nano-composites.

Please cite this article in press as: Chen L et al. Preparation, characterization and thermoelectricity of ATT/$TiO_2$/PANI nano-composites doped with different acids. Composites: Part B (2012), doi:10.1016/j.compositesb.2012.02.028

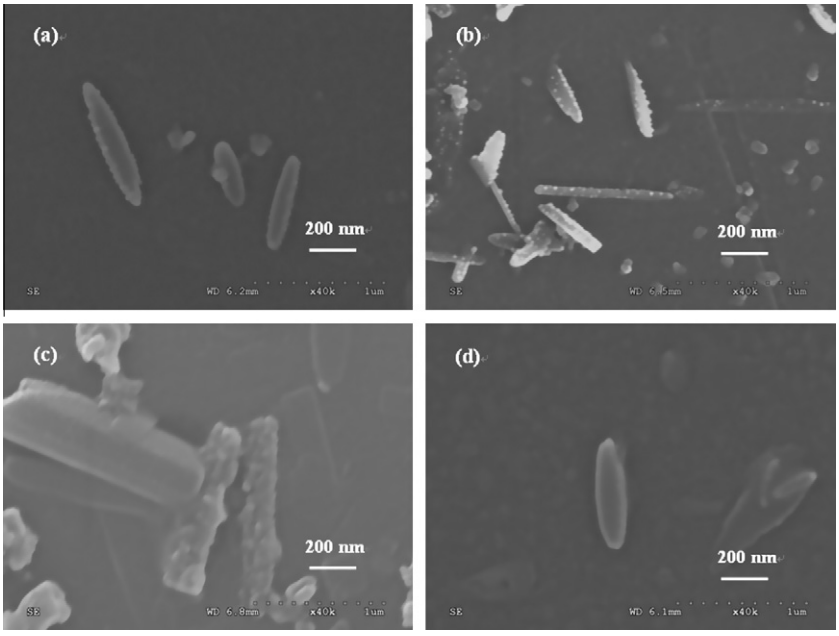


**Fig. 2.** SEM image of ATOP nano-composites. (a) ATOP-1 nano-composites; (b) ATOP-2 nano-composites; (c) ATOP-3 nano-composites; and (d) ATOP-4 nano-composites.

with a length of ~650 nm and diameter of ~100 nm, which agrees with the fact that ATT is a type of natural fibrillar silicate clay mineral. Compared with the pure ATT, the surface of samples is not smooth; and the dimensions of samples are increased. This may attribute to the extra $TiO_2$ and PANI coatings, confirming a good cladding structure.

Fig. 3 displays the XRD pattern of various acid-doped ATOP samples. Pure $TiO_2$, ATT and PANI are also listed for the comparison. It can be seen that the diffraction patterns of all ATOP samples match well with the typical patterns of ATT, PANI and $TiO_2$. The peaks at 8.56° can be observed in the doped samples, which is ascribed to {110} crystal face of ATT. The distinct peaks of $2\theta$ at 25.4°, 38°, 48.3°, 54.1°, 55.2°, 53.9°, 62.8°and 70.5° are in agreement with the standard anatase $TiO_2$ XRD spectrum. Also the distinct peaks of $2\theta$ at 15.1°, 20.8°and 25.4° agree with the standard PANI XRD spectrum, indicating the formation of PANI. Two peaks at 20.8° and 25.4° belong to periodicity parallel and perpendicular to polymer chain respectively. It is reported that there was a positive correlation between the conductivity and intensity of diffraction peaks at 25.4° [26]. However, only according to the counts of diffraction peaks at 25.4°, we cannot deduce the order of electric conductivity among various acid-doped ATOP samples because the diffraction peaks at 25.4° belongs to two different materials.

The FTIR spectra of the ATOP samples are shown in Fig. 4. The absorption band observed at 2912 $cm^{-1}$–2851 $cm^{-1}$ in the doped sample, can be ascribed to the surfactant DBSA; the absorption bands at 1676 $cm^{-1}$ and 1019 $cm^{-1}$ are assigned to the O═S═O stretching of organic acid. It should be noted that most PANI peaks of acid-doped ATOP samples are shifted to the lower wave number compared with that of the eigenstate PANI. Table 1 lists all the absorption bands in the spectra. The offset of vibration peaks can be calculated, comparing with the eigenstate PANI. The maximum offset occurs in N═Q═N bond, shifted by 22 $cm^{-1}$ (ATOP-1), 6 $cm^{-1}$ (ATOP-2), 26 $cm^{-1}$ (ATOP-3), and 18 $cm^{-1}$ (ATOP-4), respectively. This red shift phenomenon may result from conjugative effect after doped with acids. Some documents indicate that the dopants are mainly bonded with the nitrogen atoms in quinine-type. It is believed that acid-doping leads to a delocalization effect which decreases the force constant between atoms, and thus decreases the electron density on PANI chains in various levels. Similar results can be found in the published elsewhere [27].

The thermal analysis results of pure $TiO_2$, ATT, PANI and various acid-doped ATOP samples are illustrated in Fig. 5. It can be seen that the residual weight of acid-doped ATOP samples is much higher than those of pure $TiO_2$, ATT, and PANI. This means the thermal stability of ATOP samples can be improved after composite

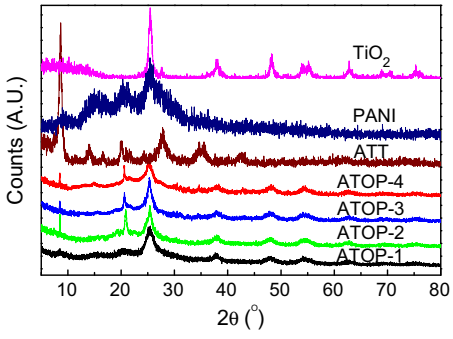


**Fig. 3.** X-ray diffraction patterns of pure ATT, PANI, $TiO_2$, and ATOP nano-composites.

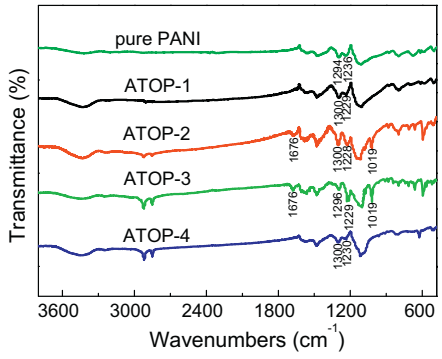


**Fig. 4.** FT-IR spectra of pure ATT, PANI, $TiO_2$, and ATOP nano-composites.

Please cite this article in press as: Chen L et al. Preparation, characterization and thermoelectricity of ATT/$TiO_2$/PANI nano-composites doped with different acids. Composites: Part B (2012), doi:10.1016/j.compositesb.2012.02.028

**Table 1**
Characteristic frequencies of eigenstate PANI and various acids doped ATOP nano-composites.

| Wavenumber ($cm^{-1}$) | | | | | Band characteristics |
|---|---|---|---|---|---|
| PANI | ATOP-1 | ATOP-2 | ATOP-3 | ATOP-4 | |
| 3435 | 3430 | 3440 | 3436 | 3434 | N=H stretching vibration |
| 1586 | 1564 | 1580 | 1560 | 1568 | N=Q=N vibration |
| 1495 | 1480 | 1480 | 1480 | 1480 | N=B=N stretching vibration |
| 1230, 1302 | 1229, 1300 | 1228, 1300 | 1229, 1296 | 1230, 1300 | Ar=N stretching |
| 1121 | 1106 | 1115 | 1103 | 1109 | C=H (Q) in of plane bending vibration |
| 827 | 798 | 798 | 798 | 798 | C=H (B) out of plane bending vibration |
| 638 | 616 | 595 | 595 | 624 | C=C (B) bending vibration |

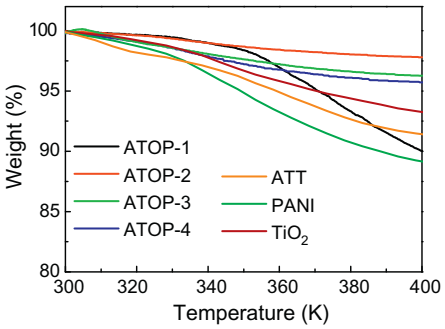


**Fig. 5.** The TG analysis of pure ATT, PANI, $TiO_2$, and ATOP nano-composites.

treatment. However, the weight loss of ATOP-1 sample is the largest, when the temperature is higher than 350 K, compared with that of other three acid-doped samples. Usually the weight loss of the samples at low temperature attribute to the removal of free water, absolute alcohol, acid and other small molecules. In fact, the weight loss of ATOP-2 sample is the minimum and that of the ATOP-3 is less. This result is in line with our expectation because hydrochloric acid is volatile; whereas organic acids and perchloric acid are less volatile. To sum up, the thermal stability of the ATOP samples doped with SSA is enhanced.

The temperature dependence of electrical conductivity ($\sigma$) of pure $TiO_2$, PANI and various acids doped ATOP samples is shown in Fig. 6. It is of interest that the ATOP nano-composites possess a higher electrical conductivity, compared with the pure $TiO_2$ and PANI. This probably originates from the compound of $TiO_2$ and PANI. On the one hand, $TiO_2$ can cause the regular arrangement of PANI chains; on the other hand, the cladding structure is conducive to electronic transfer along chain and jump between chains. Although the ATT belongs to insulator, the addition of it has no negative effect on electrical conductivity. In contrast, the electrical conductivity of ATOP samples has been improved. Moreover, it should be noted that the electrical conductivity of all the samples can reach several S/cm and exhibit a typical non-metallic temperature dependence ($d\sigma/dT > 0$) [28]. This may be ascribed to the increase of the carrier concentration after the temperature elevated; and thus increase the electrical conductivity [29,30]. In our present work, the electrical conductivity of ATOP-3 sample is the best; it reaches the maximum (6.67 S/cm), 2 times more than that of PANI (2.58 S/cm) at 373 K.

Fig. 7 shows the temperature dependence of the Seebeck coefficient ($\alpha$) for pure $TiO_2$, PANI and various acids doped ATOP samples. The Seebeck coefficient shows an opposite trend to that of electrical conductivity. The pure $TiO_2$ and PANI are proved to be n-type inorganic semiconductor and p-type organic semiconductor, respectively. The ATOP nano-composites are classified as p-type. It is encouraging to find out that the Seebeck coefficient of acid-doped ATOP samples is about 2–4 times higher than that of pure $TiO_2$ and PANI. The results are similar to the studies on PANI with different acid-doped by Liu et al. [31]. In addition, the Seebeck coefficient decreases with the temperature increasing attribute to the increase of carrier concentration [30,32]. The Seebeck coefficient of ATOP-3 sample is better than others in the range of 323–373 K; it keeps a higher value (57 μV/K) at 363 K.

The thermoelectric figure-of-merit ($ZT$) is a common measure of a material's energy conversion efficiency:

$$ZT = (\alpha^2\sigma/\kappa)T \quad (1)$$

Where $\alpha$, $\sigma$, $\kappa$, and $T$ are Seebeck coefficient, electrical conductivity, thermal conductivity and absolute temperature respectively.

The thermal conductivity of ATT is about 0.06 $Wm^{-1}K^{-1}$ and that of PANI is around 0.3 $Wm^{-1}K^{-1}$ at room temperature [33,34]. Mun et al. have reported the thermal conductivity of $TiO_2$ is 0.5 $Wm^{-1}K^{-1}$ [35]. The average thermal conductivity of ATOP nano-composites is about 0.148 $Wm^{-1}K^{-1}$. We also note that the thermal conductivity do not change significantly with the temperature increased. For example, the thermal conductivity of

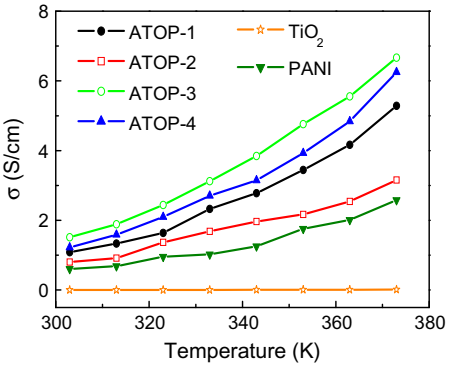


**Fig. 6.** The temperature dependence of electrical conductivity of pure $TiO_2$, PANI, and ATOP nano-composites.

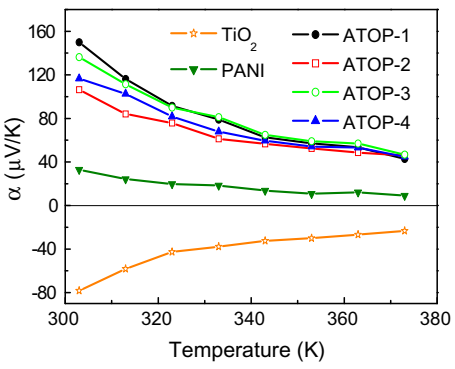


**Fig. 7.** The temperature dependence of Seebeck coefficient of pure $TiO_2$, PANI, and ATOP nano-composites.

Please cite this article in press as: Chen L et al. Preparation, characterization and thermoelectricity of ATT/$TiO_2$/PANI nano-composites doped with different acids. Composites: Part B (2012), doi:10.1016/j.compositesb.2012.02.028

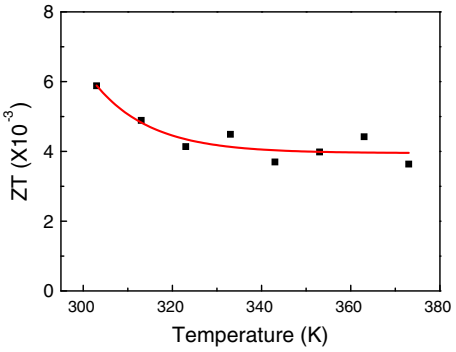


**Fig. 8.** The temperature dependence of ZT of ATOP-3 nano-composites.

ATOP-3 is about 0.155 $Wm^{-1}K^{-1}$ at 323 K, and is about 0.144 $Wm^{-1}K^{-1}$ at 373 K. This means that the addition of ATT can reduce the thermal conductivity efficiently and maintain a good stability over a wide temperature range.

The *ZT* of ATOP nano-composites can be calculated according to the Eq. (1). Fig. 8 shows the *ZT* of ATOP-3 nano-composites as a function of temperature. Though *ZT* decrease slightly with the increase of temperature, dropped from $5.88 \times 10^{-3}$ at 303 K to $3.82 \times 10^{-3}$ at 373 K, ZT still maintain a relative higher value according to our evaluation. The ZT of ATOP-3 nano-composites is several hundred times larger than that of pure $TiO_2$ and PANI, which is $0.48 \times 10^{-4}$ and $0.26 \times 10^{-4}$ at 373 K, respectively. Li et al. have reported the maximum of ZT in doped PANI is $1.2 \times 10^{-4}$ at 373 K [28]. Though the data is slight higher than our experimental, their magnitude is equivalent. Compared with the existing literature on $TiO_2$, PANI or their composites, the ZT of ATOP-3 nano-composites is the largest. We believe that HCl + SSA dual acids doped ATT/$TiO_2$/PANI nano-composites can be promising for thermoelectric applications, especially in power generation with low temperature heat, e.g. exhaust gas, terrestrial heat, solar energy, etc. Therefore, even if a little part of waster can be converted into electricity, its impact on the energy situation would be enormous.

## 4. Conclusion

Acid-doped ATOP nano-composites are of rod-like structure with a length of ~650 nm and diameter of ~100 nm. Acid-doped ATOP nano-composites possess a higher Seebeck coefficient, electrical conductivity, and a lower thermal conductivity compared with pure $TiO_2$, PANI or their composites. The electrical conductivity of ATOP-3 nano-composites can reach 6.67 S/cm at 373 K and exhibit a typical non-metallic temperature dependence. The Seebeck coefficient of ATOP-3 sample is 57 μV/K at 363 K, about 2–4 times higher than that of pure $TiO_2$ and PANI. The addition of ATT can reduce the thermal conductivity of ATOP nano-composites, and maintain a good stability over a wide temperature range. The thermal conductivity of ATOP nano-composites is about 0.148 $Wm^{-1}K^{-1}$. Compared with other samples, the ZT of HCl + SSA dual acids doped nano-composites is the largest and is several hundred times larger than that of pure $TiO_2$ and PANI. Moreover, it can maintain a relatively larger value, $3.82 \times 10^{-3}$ at 373 K. It is strongly believed that HCl + SSA dual acids doped ATOP nano-composites could be promising for power generation with low temperature heat.

## Acknowledgements

This work is supported by National Science Foundation of China (51175212), College Nature Science Foundation of Jiangsu Province (HGA1016) and partially supported by DARPA to AMRI-UNO (HR0011-08-1-0084 and W91CRB-10-C-0189). The authors would like to thanks the foundation of Qinlan Projects of Jiangsu Province 2010.

## References

[1] Tritt TM, Subramanian MA. Thermoelectric materials, phenomena, and applications: a bird's eye view. MRS Bull 2006;31(3):188–94.
[2] Snyder GJ, Toberer ES. Complex thermoelectric materials. Nat Mater 2008;7(2):105–14.
[3] Moriarty GP, Wheeler JN, Yu C, Grunlan JC. Increasing the thermoelectric power factor of polymer composites using a semiconducting stabilizer for carbon nanotubes. Carbon 2012;50(3):885–95.
[4] Zhao JC, Du FP, Zhou XP, Cui W, Wang XM, Zhu H, et al. Thermal conductive and electrical properties of polyurethane/hyperbranched poly(urea–urethane)-grafted multi-walled carbon nanotube composites. Composites Part B 2011;42(8):2111–6.
[5] Wang W, Jia FL, Huang QH, Zhang JZ. A new type of low power thermoelectric micro-generator fabricated by nanowire array thermoelectric material. Microelectron Eng 2005;77(3–4):223–9.
[6] Wang SR, Qiu JJ. Enhancing thermal conductivity of glass fiber/polymer composites through carbon nanotubes incorporation. Composites Part B 2010;41(7):533–6.
[7] Li YL, Jiang J, Xu GJ, Li W, Zhou LM, Li Y, et al. Synthesis of micro/nanostructured p-type $Bi_{0.4}Sb_{1.6}Te_3$ and its thermoelectrical properties. J Alloys Compd 2009;480(2):954–7.
[8] Su LS, Gan YX. Formation and thermoelectric property of $TiO_2$ nano tubes covered by Te-Bi-Pb nanoparticles. Electrochim Actra 2011;56(16):5794–803.
[9] Ghosh P, Siddhanta SK, Chakrabarti A. Characterization of poly(vinyl pyrrolidone) modified polyaniline prepared in stable aqueous medium. Eur Polym J 1999;35(4):699–710.
[10] Liang JZ, Li FH. Heat transfer in polymer composites filled with inorganic hollow micro-spheres: A theoretical model. Polym Test 2007;26(8):1025–30.
[11] Park OK, Kim NH, Yoo G-H, Rhee KY, Lee JH. Effects of the surface treatment on the properties of polyaniline coated carbon nanotubes/epoxy composites. Composites Part B 2010;41(1):2–7.
[12] Liang JZ. Predictions of tensile strength of short inorganic fibre reinforced polymer composites. Polym Test 2011;30(7):749–52.
[13] Vu QT, Pavlik M, Hebestreit N, Pfleger J, Rammelt U, Plieth W. Electrophoretic deposition of nanocomposites formed from polythiophene and metal oxides. Electrochim Acta 2005;51(6):1117–24.
[14] Song RY, Park JH, Sivakkumar SR, Kim SH, Ko JM, Park DY, et al. Supercapacitive properties of polyaniline/Nafion/hydrous $RuO_2$ composite electrodes. J Power Sources 2007;166(1):297–301.
[15] Li HL, Wang JX, Chu QX, Wang Z, Zhang FB, Wang SC. Theoretical and experimental specific capacitance of polyaniline in sulfuric acid. J Power Sources 2009;190(2):578–86.
[16] Mardic Z, Rokovic MK. Polyaniline as cathodic material for electrochemical energy sources: The role of morphology. Electrochim Actra 2009;54(10):2941–50.
[17] Angelopoulos M, Patel N, Saraf R. Amic acid doping of polyaniline: Characterization and resulting blends. Synth Met 1993;55(2–3):1552–7.
[18] Palaniappan S, John A, Amarnath CA, Rao VJ. Mannich-type reaction in solvent free condition using reusable polyaniline catalyst. J Mol Catal A: Chem 2004;218(1):47–53.
[19] Bernard M-C, Goff AH-L, Bich VT, Zeng W. Study by optical multichannel analysis of the electrochromic phenomena in polyaniline doped with camphorsulfonic acid. Synth Met 1996;81(2–3):215–9.
[20] Chen SA, Fang Y, Lee HT. Polyacrylic acid-doped polyaniline as p-type semiconductor in Schottky barrier electronic device. Synth Met 1993;57(1):4082–6.
[21] Chen LL, Ding HY, Zhang Y, Zhou GH. Synthesis and characterization on ATP/$TiO_2$/PANI core-shell nanocomposites. Adv Mater Res 2011;282–283(1):354–8.
[22] Aysegul U, Orhan T, Songul S, Ersay E, Ayse GY, Gokhan GB. The electrical conductivity properties of polythiophene/$TiO_2$ nano-composites prepared in the presence of surfactants. Curr Appl 2009;9(4):866–71.
[23] Olphen VH, Fripiat JJ. Data-handbook for clay materials and non-metallic minerals. New York: Pergramon press; 1977.
[24] Yang C, Liu P. Core-shell attapulgite@polypyrrole composite with well-defined corn cob-like morphology via self-assembling and in situ oxidative polymerization. Synth Met 2009;159(19–20):2056–62.
[25] Wang LH, Sheng J. Preparation and properties of polypropylene/org-attapulgite nanocomposites. Polymer 2005;46(16):6243–9.
[26] Moon YB, Cao Y, Smith P, Heeger AJ. X-ray diffraction of polyaniline. Polym Commun 1989;30(2):196–9.
[27] Stafstirom S, Bredal JL. Evolution of structure and electronic properties in oxidized polyaniline as a function of the torsion angle between adjacent rings. Synth Met 1986;14(4):297–308.
[28] Li JJ, Tang XF, Li H, Yan YG, Zhang QJ. Synthesis and thermoelectric properties of hydrochloric acid-doped polyaniline. Synth Met 2010;160(11–12):1153–8.

Please cite this article in press as: Chen L et al. Preparation, characterization and thermoelectricity of ATT/$TiO_2$/PANI nano-composites doped with different acids. Composites: Part B (2012), doi:10.1016/j.compositesb.2012.02.028

[29] Du Y, Shen SZ, Cai KF, Casey PS. Research progress on polymer–inorganic thermoelectric nanocomposite materials. Prog Polym Sci <http://dx.doi.org/10.1016/j.progpolymsci.2011.11.003>.
[30] Zhu PW, Imai Y, Isoda Y, Shinohara Y, Jia XP, Zou GT. Carrier-Concentration-Dependent Transport and Thermoelectric Properties of PbTe Doped with Sb2Te3. Mater Trans 2005;46(12):2690–3.
[31] Liu J, He L, Zhang LM. Study on thermoelectric properties of polyaniline. J Huazhong Univ of Sci Tech 2003;31(4):73–5.
[32] Mateeva N, Niculescu H, Schlenoff J, Testardi LR. Correlation of seebeck coefficient and electric conductivity in polyaniline and polypyrrole. J Appl Phys 1998;83(6):3111–7.
[33] De Albuquerque JE, Melo WLB, Faria RM. Determination of physical parameters of conducting polymers by photothermal spectroscopies. Rev Sci Instrum 2003;74(1):306–8.
[34] Sun YM, Wei ZM, Xu W, Zhu DB. A three-in-one improvement in thermoelectric properties of polyaniline brought by nanostructures. Synth Met 2010;160(21–22):2371–6.
[35] Maekawa T, Kurosaki K, Tanaka T, Yamanaka S. Thermal conductivity of titanium dioxide films grown by metal-organic chemical vapor deposition. Surf Coat Technol 2008;202(13):3067–71.

Please cite this article in press as: Chen L et al. Preparation, characterization and thermoelectricity of ATT/$TiO_2$/PANI nano-composites doped with different acids. Composites: Part B (2012), doi:10.1016/j.compositesb.2012.02.028